

Supporting Information

Tough, frost resistant and high adhesive eutectic ionogel prepared by constructing high-density hydrogen bond network

Li Jina, Su Jua, Yiming Zhaoa, Suli Xinga, Jun Tanga, Yonglyu Hea, Chen Chena, Gengyuan Liang^b, Jianwei Zhang^{a*}

^a College of Aerospace Science and Engineering, National University of Defense Technology, Changsha 410073, China

^b High Speed Aerodynamics Institute, China Aerodynamics Research and Development Center, Mianyang 621000, China.

* Corresponding author:

J. Zhang, E-mail: jianwei_zhang@nudt.edu.cn

G. Liang, E-mail: lgy940612@163.com

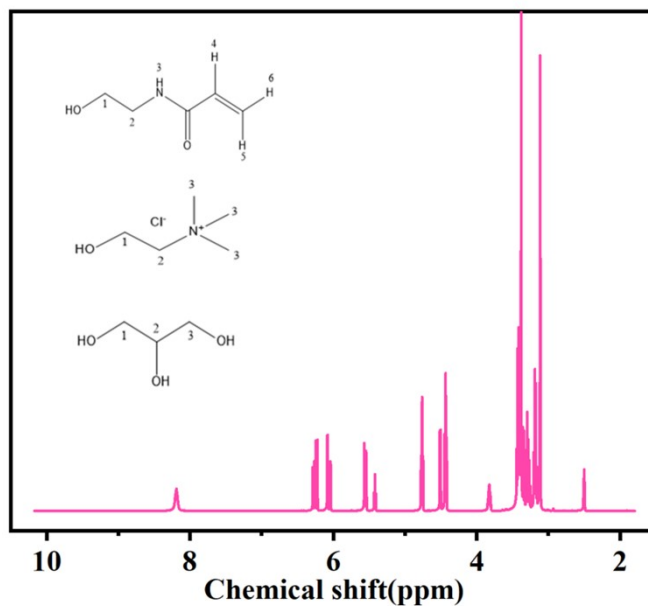


Fig.S1 ¹H NMR of ChCl-NHEMAA precursor solutions.

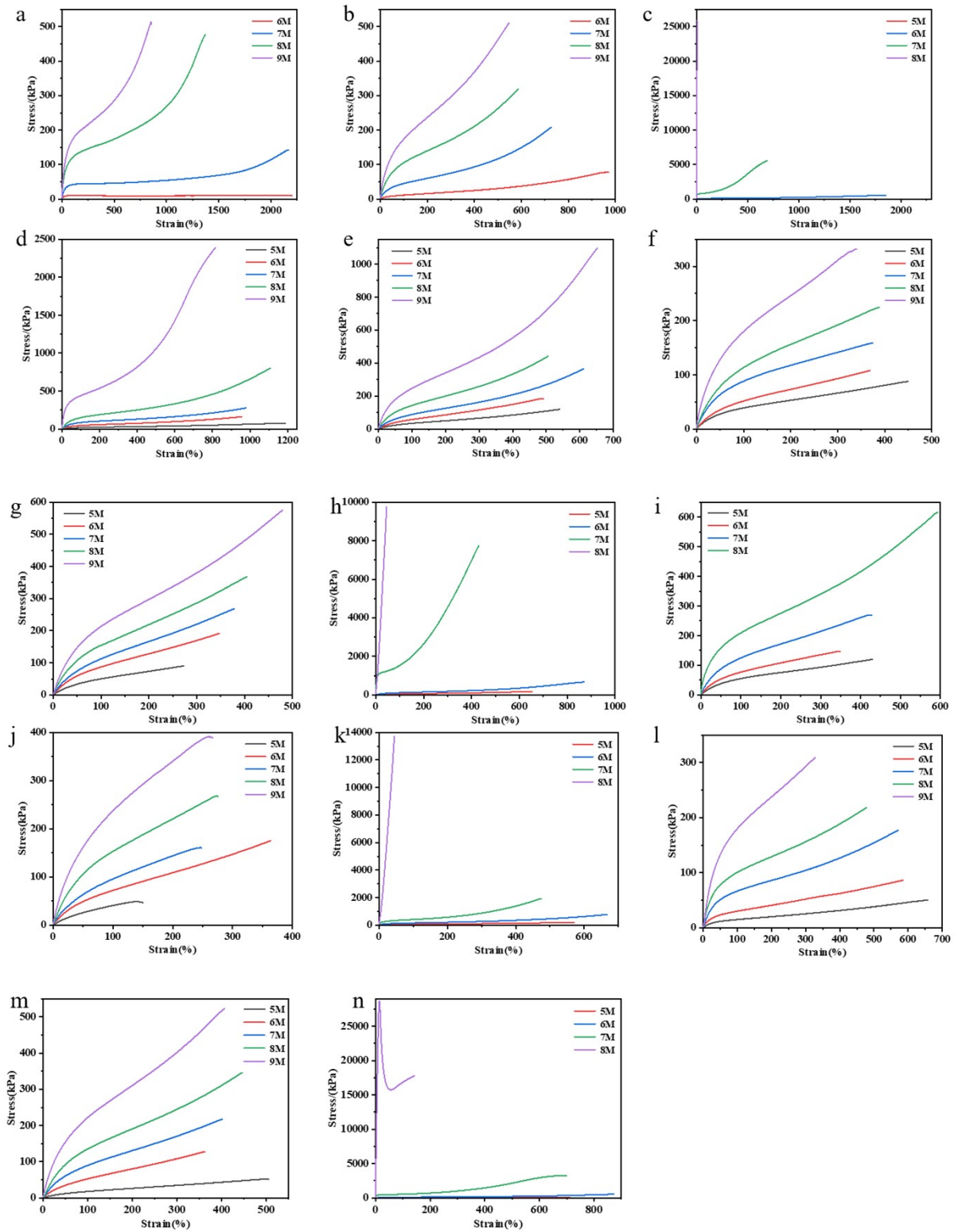


Fig.S2 a) Stress-strain curve of ionogel of ChLA-AA system; b) Stress-strain curve of ionogel of ChLA-HEA system; c) Stress-strain curve of ionogel of ChLA-NHEMAA system; d) Stress-strain curve of ionogel of ChGly-AA system; e) Stress-strain curve of ionogel of ChGly-HEA system; f) Stress-strain curve of ionogel of ChAc-AA system; g) Stress-strain curve of ionogel of ChAc-HEA system; h) Stress-strain curve of ionogel of ChAc-NHEMAA system; i) Stress-strain curve of ionogel of ChAc-Gly system; j) Stress-strain curve of ionogel of ChAc-Gly system; k) Stress-strain curve of ionogel of ChAc-Gly system; l) Stress-strain curve of ionogel of ChAc-Gly system; m) Stress-strain curve of ionogel of ChAc-Gly system; n) Stress-strain curve of ionogel of ChAc-Gly system.

HEA system; h) Stress strain-curve of ionogel of ChAc-NHEMAA system; i) Stress-strain curve of ionogel of Churea-AA system; j) Stress-strain curve of ionogel of Churea-HEA system; k) Stress-strain curve of ionogel of Churea-NHEMAA system; l) Stress-strain curve of ionogel of ChEG-AA system; m) Stress-strain curve of ionogel of ChEG-HEA system; n) Stress-strain curve of ionogel of ChEG-NHEMAA system.

Note: **a.** ChLA-AA-5 and ChLA-HEA-5 cannot test their stress-strain curves due to their high viscosity. **b.** ChLA-NHEMAA-9, ChAc-NHEMAA-9, Churea-NHEMAA-9 and ChEG-NHEMAA-9 were unable to test their stress-strain curves due to brittle fracture caused by excessive strength while demolding. **c.** Churea-AA-9 was unable to test its stress-strain curve due to burst aggregation during the synthesis process. The tensile speed is 100 mm/min.

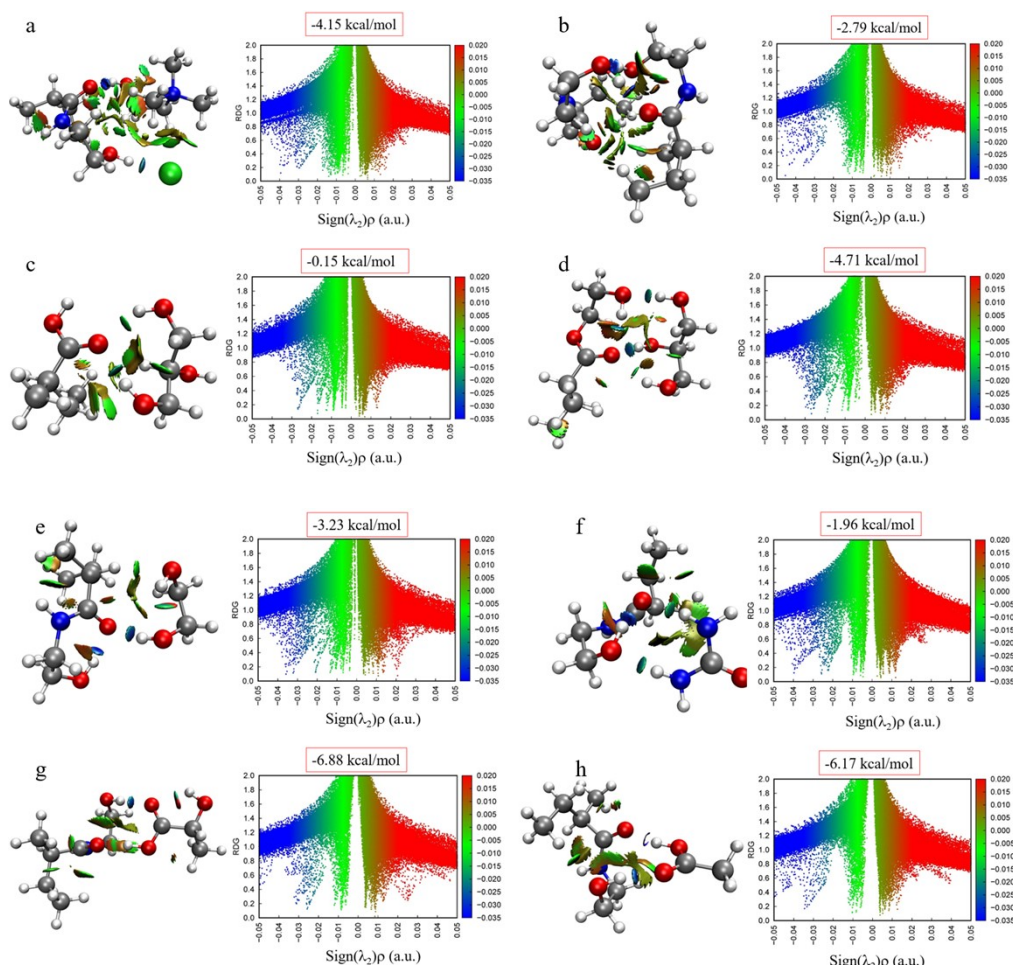


Fig.S3 a) Colour-filled RDG plots (isovalue=0.5) and RDG vs $\text{sign}(\lambda_2)\rho$ of Chcl/NHEMAA; b) Colour-filled RDG plots (isovalue=0.5) and RDG vs $\text{sign}(\lambda_2)\rho$ of NHEMAA/NHEMAA; c)

Colour-filled RDG plots (isovalue=0.5) and RDG vs sign(λ_2) ρ of AA/Gly; d) Colour-filled RDG plots (isovalue=0.5) and RDG vs sign(λ_2) ρ of HEA/Gly; e) Colour-filled RDG plots (isovalue=0.5) and RDG vs sign(λ_2) ρ of NHEMAA/EG; f) Colour-filled RDG plots (isovalue=0.5) and RDG vs sign(λ_2) ρ of NHEMAA/urea; g) Colour-filled RDG plots (isovalue=0.5) and RDG vs sign(λ_2) ρ of NHEMAA/LA; h) Colour-filled RDG plots (isovalue=0.5) and RDG vs sign(λ_2) ρ of NHEMAA/Ac. The color bar shows that blue, green, and red represent strong attraction interactions (hydrogen bonding), van der Waals interactions, and strong nonbonded overlap, respectively.

All calculations were carried out with the Gaussian 16 software [1]. Density functional theory (DFT) calculations were carried out with the B3LYP functional [2] with the combination of Grimme's D3BJ [3] version of dispersion correction. For geometry optimization, the 6-31G(d,p) basis set and IEFPCM [4] solvent model for Tetrahydrofuran were used. The frequencies were computed analytically at the same level of theory as the geometry optimizations to identify the nature of all stationary points being minimum (no imaginary frequency) and also to obtain the Gibbs free energy correction at 298.15 K. The final and solvation energies for the fully optimized structures in the Tetrahydrofuran were calculated by employing the SMD [5] continuum solvation model with the larger 6-311(d, p) basis set. The binding energy (E_b) was calculated by the following equation:

$$E_b = E_{Complex} - (E_{M1} + E_{M2}) \#(1)$$

where $E_{Complex}$, E_{M1} , and E_{M2} represent the energies of the complex, and energies of the interacting molecules, respectively. The combined conformation search using xtb[6] and molclus software.

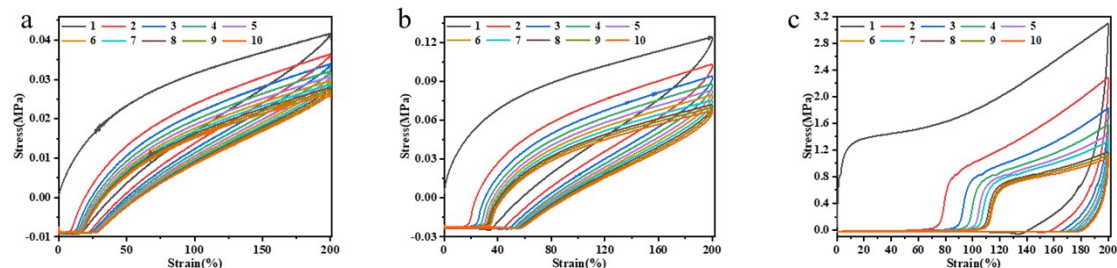


Fig.S4 a) Cyclic stress-strain curve of ChGly-NHEMAA-5 under 10 consecutive tensile tests at 200% strain; b) Cyclic stress-strain curve of ChGly-NHEMAA-6 under 10 consecutive tensile tests at 200% strain; c) Cyclic stress-strain curve of ChGly-NHEMAA-7 under 10 consecutive tensile tests at 200% strain.

Note: The tensile speed is 100 mm/min.

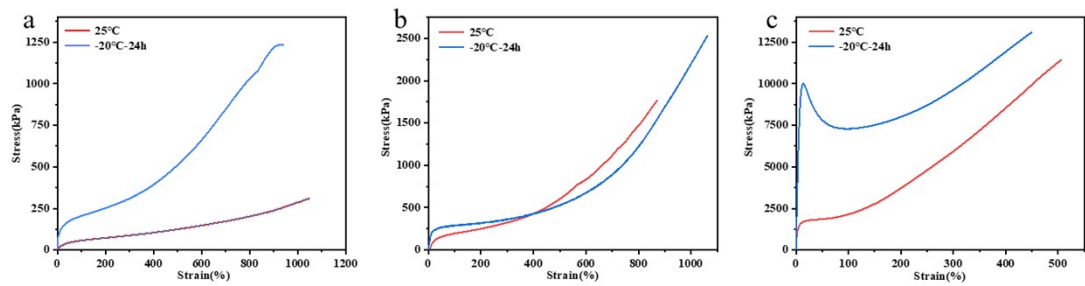


Fig.S5 a) Stress-strain curve of ChGly NHEMAA-5 after freezing at -20 °C for 24 hours; b) Stress-strain curve of ChGly NHEMAA-6 after freezing at -20 °C for 24 hours; c) Stress-strain curve of ChGly NHEMAA-7 after freezing at -20 °C for 24 hours.

Note: The tensile speed is 100 mm/min.

References:

- [1]. Frisch, M. J.; Trucks, G. W.; Schlegel, H. B.; Scuseria, G. E.; Robb, M. A.; Cheeseman, J. R.; Scalmani, G.; Barone, V.; Petersson, G. A.; Nakatsuji, H.; Li, X.; Caricato, M.; Marenich, A. V.; Bloino, J.; Janesko, B. G.; Gomperts, R.; Mennucci, B.; Hratchian, H. P.; Ortiz, J. V.; Izmaylov, A. F.; Sonnenberg, J. L.; Williams, Ding, F.; Lipparini, F.; Egidi, F.; Goings, J.; Peng, B.; Petrone, A.; Henderson, T.; Ranasinghe, D.; Zakrzewski, V. G.; Gao, J.; Rega, N.; Zheng, G.; Liang, W.; Hada, M.; Ehara, M.; Toyota, K.; Fukuda, R.; Hasegawa, J.; Ishida, M.; Nakajima, T.; Honda, Y.; Kitao, O.; Nakai, H.; Vreven, T.; Throssell, K.; Montgomery Jr., J. A.; Peralta, J. E.; Ogliaro, F.; Bearpark, M. J.; Heyd, J. J.; Brothers, E. N.; Kudin, K. N.; Staroverov, V. N.; Keith, T. A.; Kobayashi, R.; Normand, J.; Raghavachari, K.; Rendell, A. P.; Burant, J. C.; Iyengar, S. S.; Tomasi, J.; Cossi, M.; Millam, J. M.; Klene, M.; Adamo, C.; Cammi, R.; Ochterski, J. W.; Martin, R. L.; Morokuma, K.; Farkas, O.; Foresman, J. B.; Fox, D. J. Gaussian 16 Rev. A.01, Wallingford, CT, 2016.
- [2]. Becke, A., Assessment of a long-range corrected hybrid functional. *J. Chem. Phys.* 1993, 98 (7), 5648-5652.
- [3]. Grimme, S.; Ehrlich, S.; Goerigk, L., Effect of the damping function in dispersion corrected density functional theory. *J. Comput. Chem.* 2011, 32 (7), 1456-1465.
- [4]. Miertuš, S.; Scrocco, E.; Tomasi, J., Electrostatic interaction of a solute with a continuum. A direct utilization of AB initio molecular potentials for the prediction of solvent effects. *Chem. Phys.* 1981, 55 (1), 117-129.
- [5]. Marenich, A. V.; Cramer, C. J.; Truhlar, D. G., Universal solvation model based on solute electron density and on a continuum model of the solvent defined by the bulk dielectric constant and atomic surface tensions. *J. Phys. Chem. B* 2009, 113 (18), 6378-6396.
- [6]. Bannwarth, C.; Ehlert, S.; Grimme, S., GFN2-xTB—An Accurate and Broadly Parametrized Self-Consistent Tight-Binding Quantum Chemical Method with Multipole Electrostatics and Density-Dependent Dispersion Contributions. *J. Chem. Theory Comput.* 2019, 15 (3), 1652-1671. Capability, Remodifiability, and Reusability, *ACS Applied Materials & Interfaces* 10(50) (2018) 44000-44010.